Task Decoupled Framework for Reference-based Super-Resolution

Yixuan Huang[1*], Xiaoyun Zhang[1*†], Yu Fu[1], Siheng Chen[1,2], Ya Zhang[1,2], Yanfeng Wang[1,2 †], Dazhi He[1]
[1]Cooperative Medianet Innovation Center, Shanghai Jiao Tong University, [2]Shanghai AI Laboratory
{huangyixuan,xiaoyun.zhang,fyuu11,sihengc,ya_zhang,wangyanfeng,hedazhi}@sjtu.edu.cn

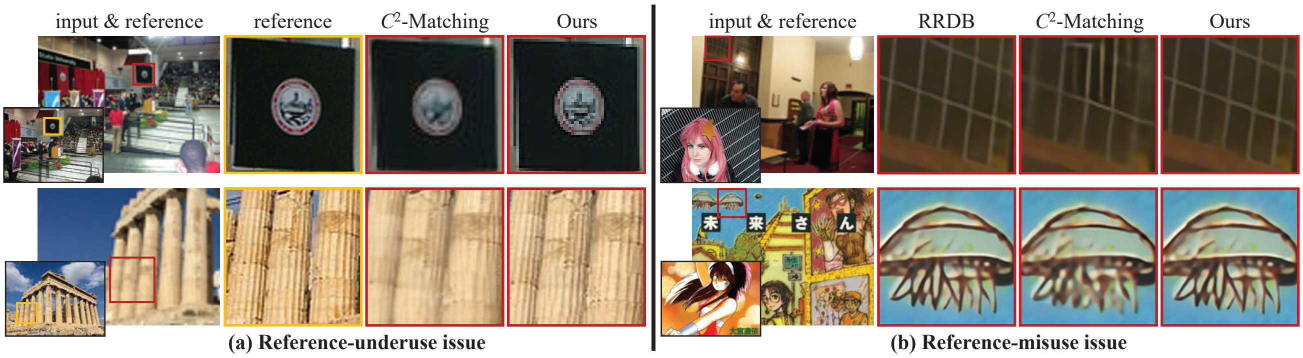

Figure 1. **Current state-of-the-art RefSR methods suffer from (a) reference-underuse issue and (b) reference-misuse issue** due to the improper coupled framework. Specifically, for the reference-underuse issue, RefSR methods transfer the detail textures from reference insufficiently, even when the reference has highly similar content to input. As for the reference-misuse issue, current methods introduce blur and artifacts, which is even worse than SISR methods, when the reference has no relevant content. Our novel task decoupled framework for RefSR mitigates these issues.

Abstract

Reference-based super-resolution(RefSR) has achieved impressive progress on the recovery of high-frequency details thanks to an additional reference high-resolution(HR) image input. Although the superiority compared with Single-Image Super-Resolution(SISR), existing RefSR methods easily result in the reference-underuse issue and the reference-misuse as shown in Fig.1. In this work, we deeply investigate the cause of the two issues and further propose a novel framework to mitigate them. Our studies find that the issues are mostly due to the improper coupled framework design of current methods. Those methods conduct the ***super-resolution task*** *of the input low-resolution(LR) image and the* ***texture transfer task*** *from the reference image together in one module, easily introducing the interference between LR and reference features. Inspired by this finding, we propose a novel framework, which decouples the two tasks of RefSR, eliminating the interference between the LR image and the reference image. The super-resolution task upsamples the LR image leveraging only the LR image itself. The texture transfer task extracts and transfers abundant textures from the reference image to the coarsely upsampled result of the super-resolution task. Extensive experiments demonstrate clear improvements in both quantitative and qualitative evaluations over state-of-the-art methods.*

1. Introduction

The goal of Single Image Super-Resolution(SISR) [10, 16, 26, 38] is to recover the high-resolution(HR) details of the image from its low-resolution(LR) counterpart. It has been widely used in image enhancement, video surveillance and remote sensing imaging. The ill-pose essence of SISR makes it easily resulting in visual artifacts as the scale factor is large(×4). To tackle the problem, Reference-based Super-Resolution(RefSR) has attracted much attention recently. Compared with SISR that only uses one single LR input, RefSR [13, 22, 27, 36, 40, 41] super-resolves the LR image with an additional HR reference image, which can provide abundant real textures for the super-resolved image. RefSR can be applied to plenty of scenarios, such as dual-cameras [31] and video streaming [25].

Current RefSR methods mostly transfer the textures based on the alignment between reference and LR images, such as spatial alignment [27, 41] and patch matching [13, 22, 36, 40]. After alignment, RefSR methods concatenate the LR and aligned reference features as the input and transfer the detailed textures to the output through some well-designed architectures, such as attention mechanism [36] and spatial adaptation module [22].

Although superior of the performance compared with SISR, current methods are easily plagued by the reference-underuse issue(*i.e.*, reference textures are transferred insuf-

[*] Equal contribution(co-first authors).
[†] Corresponding author.

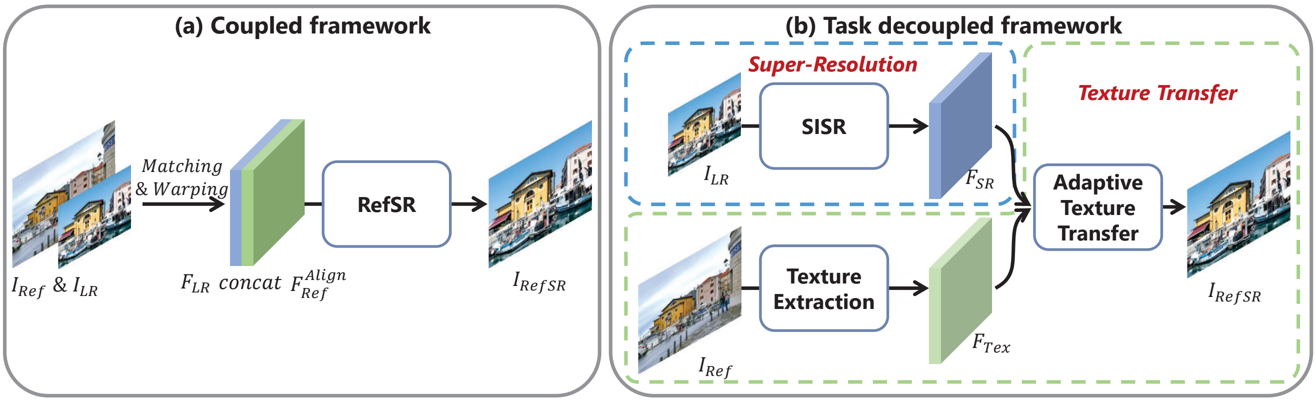

Figure 2. **Framework Comparison. (a)** After the alignment between LR and reference, previous coupled framework uses a single network to process the super-resolution of LR input and texture transfer at the same time, which easily introduces interference between LR and reference images, resulting in reference-underuse issue and reference-misuse issue as shown in Fig.1. **(b)** Our framework decouples the RefSR process into super-resolution of LR image and texture transfer. In the super-resolution, we super-solve the LR input independently of the reference. In the texture transfer, we extract the texture information from reference, then transfer the detailed textures to the coarsely upsampled result.

ficiently) and the reference-misuse issue(*i.e.*, irrelevant reference content deteriorates the results) as shown in Fig.1. The two issues are mainly due to the inadequate framework design of current RefSR methods, which couple the super-resolution task of the LR image and the texture transfer task from the reference image in one single module. As shown in Fig.2(a), most RefSR methods design a single module to execute the super-resolution task and the texture transfer task, using the concatenation of LR features and aligned reference features as the input. Processing the LR and reference images simultaneously with convolution operation will introduce disturbance to each other. Specifically, on the one hand, if the reference is highly similar to the input LR image, the model should concentrate more on transferring the aligned reference features to the output. However, the texture transfer process can be interfered by the input LR image and result in the reference-underuse issue, in which the model outputs the average of the aligned reference image and the LR image, as shown in Fig.1(a). On the other hand, as the reference content is irrelevant to the LR input image, the incongruous reference will disturb the super-resolution task of the LR image, when processing the LR and reference images at the same time, which results in the reference-misuse issue as shown in Fig.1(b).

To handle the two issues, as shown in Fig.2 (b), we propose a novel framework for RefSR based on decoupling the super-resolution task and the texture transfer task of RefSR. The decoupled task of the super-resolution aims to super-resolve the LR image coarsely without the disturbance of the reference image. The texture transfer task is to extract the textures from the reference image and further transfer the detailed textures to the result of the super-resolution task. In addition, in order to extract and transfer abundant textures stably from the reference, we propose the texture extraction module and the adaptive texture transfer module. On five benchmark datasets, CUFED5, Sun80, Urban100, Manga109 and WR-SR, the experiment shows that the performance of our method exceeds state-of-the-art methods both quantitatively and qualitatively.

To summarize, our contributions include:

- We deeply investigate the cause of the reference-underuse issue and the reference-misuse issue for RefSR. The two issues are mainly due to the improper coupled framework of current RefSR methods.
- To tackle the two issues, we propose a novel framework for RefSR based on decoupling the super-resolution task and the texture transfer task. The super-resolution task upsamples the LR image independently, and the texture transfer task extracts and transfers textures from the reference image.
- Experimental results demonstrate that our proposed method significantly outperforms the existing RefSR methods both quantitatively and qualitatively.

2. Related Work

Single Image Super-Resolution. Single Image Super-Resolution(SISR) aims to recover the HR image with just a single LR image as input. In recent years, deep learning based methods [9, 10, 15–17, 20, 21, 26, 29, 38, 39] have achieved excellent performance on the SISR task. However, most of them obtain over-smooth images because of the mean square(MSE) loss. To improve the visual quality, perceptual loss [14] and adversarial loss [18, 33, 37] are proposed. Although perceptual loss and adversarial loss improve the visual quality, the methods can easily result in hallucinations and artifacts.

Reference-based Image Super-Resolution. The goal of Reference-based Image Super-Resolution(RefSR) [22,

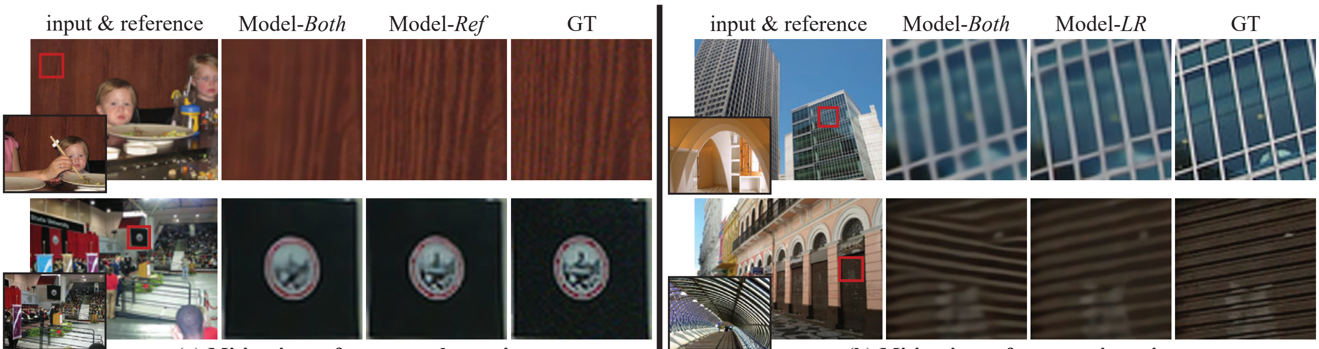

(a) Mitigating reference-underuse issue

(b) Mitigating reference-misuse issue

Figure 3. **Removal of the interference between the LR image and the reference image mitigates the reference-underuse and reference-misuse issues.** (a) When we remove the LR image input, the Model-Ref transfers more textures from the relevant high quality reference. (b) When we remove the irrelevant reference, the Model-LR overcomes the blur and artifacts caused by reference interference.

27, 34–36, 40, 41] is to super-solve the LR image with an additional reference HR image, while single image super-resolution only uses the LR image. We can obtain the reference through image retrieval methods [6]. The RefSR methods transfer the textures from the reference image through the alignment between the LR and reference images. CrossNet [41] aligned the reference and LR images by the flow estimation between two images. SSEN [27] further used deformable convolution to extract the reference features instead. However, the fatal limitation of the above spatial alignment methods is that they all lack the ability to build the long-distance correlation of two different images. Therefore, patch matching based methods [13, 22, 36, 40] are proposed. SRNTT [40] operated the patch matching on multi-scale features and then transferred the texture information into LR images. Transformer architecture has been introduced into RefSR in TTSR [36], and the hard attention and soft attention can extract reference features more properly. MASA [22] proposed a spatial adaptation module to solve the potential large disparity in distributions between LR and reference images. To match the images explicitly, C^2-Matching [13] introduced contrastive learning and knowledge distillation into patch matching steps, overcoming the transformation gap between LR and Ref images.

However, most current RefSR methods are designed to upsample the LR image and transfer textures from the reference image through a single module simultaneously, which easily results in the reference-underuse issue and the reference-misuse issue as shown in Fig.1. In contrast, our framework decouples the super-resolution task and the texture transfer task of RefSR, excluding the interference between the LR image and the reference image, thus solving the two issues to a large extent.

3. Analysis of the RefSR framework

3.1. Coupled framework for RefSR

Given a LR image $\mathbf{I}_{LR}$ as the input, Reference-based Super-Resolution(RefSR) aims to produce the high-resolution image $\mathbf{I}_{RefSR}$ with the guidance of an additional HR reference image $\mathbf{I}_{Ref}$. As shown in Fig.2(a), the framework of most existing methods [13, 22, 36, 40] can be summarized as the coupled framework. The coupled framework firstly makes the alignment between $\mathbf{I}_{LR}$ and $\mathbf{I}_{Ref}$, obtaining the LR features $\mathbf{F}_{LR}$ and aligned reference features $\mathbf{F}_{Ref}^{align}$, and then reconstruct the HR image:

$$\mathbf{I}_{RefSR} = \mathcal{G}([\mathbf{F}_{LR}, \mathbf{F}_{Ref}^{align}]), \tag{1}$$

where $\mathcal{G}$ denotes the RefSR network, and $[,]$ denotes the concatenation operation.

3.2. Analysis of the reference-underuse issue and the reference-misuse issue

The coupled framework easily results in the reference-underuse issue and the reference-misuse issue, due to the interference between the LR image and the reference image. Therefore, we're curious about whether the two issues can be tackled by separating the process of the LR and reference images. To further investigate the two issues, we retrain the C^2-Matching [13] model, which is the state-of-the-art method recently, for the following settings:

- Model-Ref: Only the aligned reference image is input to reconstruct the final HR image without the LR image. So the model only processes the texture transfer task from the reference image.
- Model-LR: Only the LR image is input to reconstruct the SR image without reference image. So the model turns into a SISR model with single image input.
- Model-$Both$: Both the LR image and aligned reference image are input to reconstruct the final HR image.

Reference-underuse issue. As shown in Fig.3(a), when similar reference images are given, the results of Model-Ref, which only use the reference image, have more similar detailed textures to the ground-truth images than Model-$Both$, which input both the LR image and reference image. The experiments demonstrate that the model can transfer the textures more sufficiently from the reference image

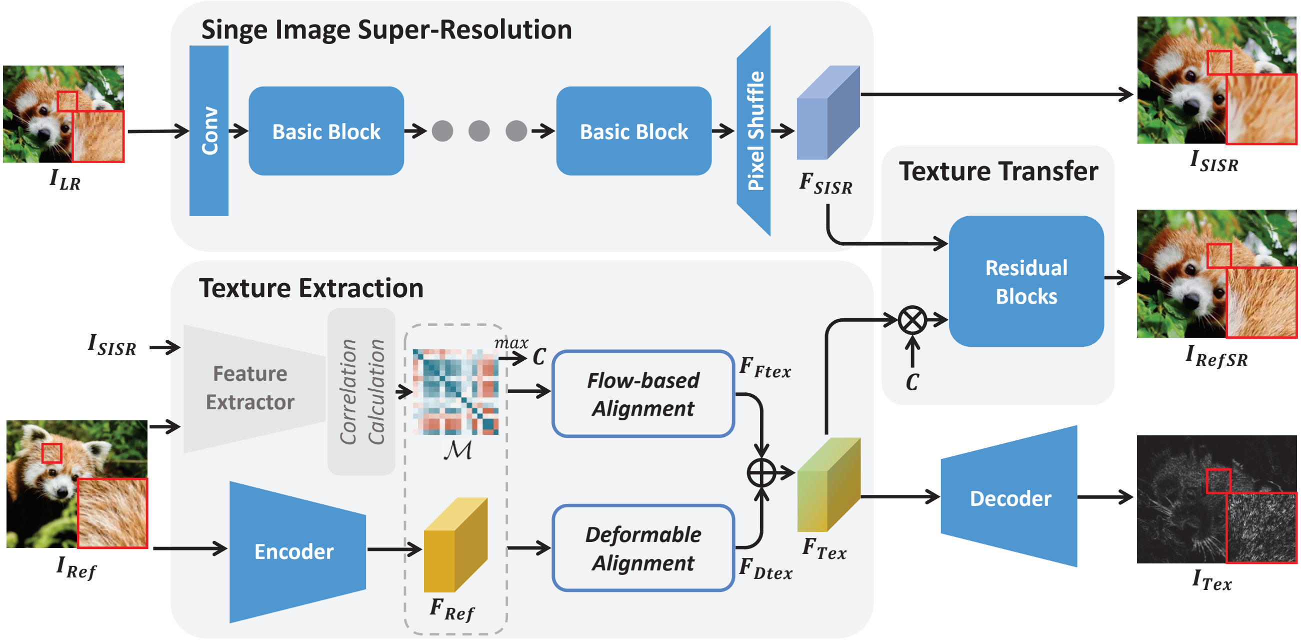

Figure 4. **Task decoupled framework overview**. For the **Super-Resolution task**, the single image super-resolution network upsamples the input image $\mathbf{I}_{LR}$ to the high-resolution image $\mathbf{I}_{SISR}$ and obtains its feature $\mathbf{F}_{SISR}$, while ensuring the structure and content information. For the **Texture Transfer task**, we first calculate the spatial correlation matrix $\mathcal{M}$ between $\mathbf{I}_{SISR}$ and the reference image $\mathbf{I}_{Ref}$. Based on the spatial correlation matrix $\mathcal{M}$, we use the texture extraction module to extract texture feature $\mathbf{F}_{Tex}$ from $\mathbf{I}_{Ref}$ through two different methods of alignment, flow-based alignment and deformable alignment. Finally, the adaptive texture transfer module transfers the detailed textures $\mathbf{F}_{Tex}$ to $\mathbf{F}_{SISR}$, and gets the final output image $\mathbf{I}_{RefSR}$.

when removing the interference of the input LR image. To a large extent, the removal of the LR image mitigates the reference-underuse issue.

Reference-misuse issue. As shown in Fig.3(b), when irrelevant reference images are given, Model-LR eliminates the blur and artifacts of the Model-$Both$ results. Therefore, by removing the influence of the incongruous reference content, the RefSR model can upsample the LR image better. The removal of the irrelevant reference mitigates the reference-misuse issue.

In conclusion, as we separate the super-resolution and the texture transfer process of RefSR, the reference-underuse issue and the reference-misuse issue are both mitigated by a large margin. Therefore, inspired by this finding, we design a novel framework based on decoupling the super-resolution task and the texture transfer task for RefSR.

4. Our Approach

4.1. Overview

In this work, to tackle the reference-underuse issue and the reference-misuse issue, we propose a novel framework based on decoupling the super-resolution task and texture transfer task of RefSR. We set two different missions for the input and reference images. Specifically, The input LR image is expected to provide the structure and content information for the final output, while the reference HR image should supply additional detailed textures. Consequently, we utilize the input LR image I_{LR} and the reference image I_{Ref} separately and integrate them subsequently. The overview of our proposed framework is shown in Fig.4, which consists of two major parts:

For the **Super-Resolution** task, we upsample the input LR image by itself without any interference from the reference image, obtaining an initial high-resolution image $\mathbf{I}_{SISR}$ and its features $\mathbf{F}_{SISR}$:

$$\mathbf{F}_{SISR} = \mathcal{F}_{SR}(\mathbf{I}_{LR}), \tag{2}$$

where $\mathcal{F}_{SR}$ denotes the SISR model, in which we use RRDB [33] as the basic block.

As for **Texture Transfer** task, we extract and transfer the fine texture feature from the reference image to the SISR feature $\mathbf{F}_{SISR}$. We first extract the reference texture feature $\mathbf{F}_{Tex}$ through the texture extraction module:

$$\mathbf{F}_{Tex} = \mathcal{F}_{TE}(\mathbf{I}_{Ref}, \mathbf{I}_{SISR}), \tag{3}$$

where $\mathcal{F}_{TE}$ denotes the texture extraction module. It's worth noting that $\mathbf{I}_{SISR}$ is only used for calculating the spatial correlation between the reference image and the input LR image. Then the textures $\mathbf{F}_{Tex}$ are transferred to $\mathbf{F}_{SISR}$ by the adaptive texture transfer module according to the similarity between the reference image and the LR input image, obtaining the final RefSR output $\mathbf{I}_{RefSR}$:

$$\mathbf{I}_{RefSR} = \mathcal{F}_{ATT}(\mathbf{F}_{Tex}, \mathbf{F}_{SISR}), \tag{4}$$

where $\mathcal{F}_{ATT}$ denotes the adaptive texture transfer module.

4.2. Texture Extraction with Alignment

The key task of texture extraction is how to process the spatial alignment of the reference image $\mathbf{I}_{Ref} \in \mathbb{R}^{H' \times W' \times 3}$ with the SISR image $\mathbf{I}_{SISR} \in \mathbb{R}^{H \times W \times 3}$. In the alignment module, we use two feature extractors to map $\mathbf{I}_{SISR}$ and $\mathbf{I}_{Ref}$ into the same feature space. The architecture of the two feature extractors are shared. After that, we use the operation of patch matching [40] in the feature space to calculate the spatial correlation map $\mathcal{M} \in \mathbb{R}^{HW \times H'W'}$ between $\mathbf{I}_{SISR}$ and $\mathbf{I}_{Ref}$. Then We calculate the index map P and confidence map C from the correlation matrix $\mathcal{M}$:

$$P_i = \arg\max_j \mathcal{M}_{i,j}, \quad C_i = \max_j \mathcal{M}_{i,j}. \tag{5}$$

The index map P can be regarded as flow information between $\mathbf{I}_{SISR}$ and $\mathbf{I}_{Ref}$. Inspired by the video super-resolution task [3, 5, 30, 32] and the video frame interpolation task [1, 2, 7, 19], we use two different methods for alignment. The first method is flow-based warping. Regarded P as the flow map, we process the backwarp operation on the $\mathbf{F}_{Ref}$ to get the aligned features. The second method is deformable [8] alignment. Previous studies [4] have shown that deformable alignment has significant improvements over flow-based alignment because of the offset diversity. However, the training of deformable alignment is unstable, which can cause offset overflow [4] thus limiting the performance. To overcome the instability of deformable alignment, we combine deformable alignment and flow-based alignment. The combination of two methods utilizes the offset diversity in deformable alignment and the stability of flow-based alignment.

Flow-based Alignment. Given the flow information P, we directly warp the feature maps $\mathbf{F}_{Ref}$ to get the $\mathbf{F}_{Ftex}$ following [22, 36, 40]:

$$\mathbf{F}_{Ftex} = \mathcal{W}(\mathbf{F}_{Ref}, P), \tag{6}$$

Where $\mathcal{W}$ denotes the operation of spatial warping.

Deformable Alignment. For the difficulty to train the deformable convolution(DCN), illuminated by the usage of deformable convolution [5,32] in the video super-resolution task, we employ optical flow to guide deformable alignment like [5]. The result of spatial warping $\mathbf{F}_{Ftex}$ is utilized to estimate the offsets o and modulation masks m for DCN:

$$o = P + \mathcal{E}_o(\mathbf{F}_{Ftex}, \mathbf{F}_{SISR}), \tag{7}$$

$$m = \sigma(\mathcal{E}_m(\mathbf{F}_{Ftex}, \mathbf{F}_{SISR})), \tag{8}$$

where $\mathcal{E}_o$ and $\mathcal{E}_m$ denote the stacks of convolution layers, and σ denotes the sigmoid function. Then we employ DCN on $\mathbf{F}_{Ref}$ to get the aligned feature $\mathbf{F}_{Dtex}$:

$$\mathbf{F}_{Dtex} = \mathcal{D}(\mathbf{F}_{Ref}, o, m), \tag{9}$$

where $\mathcal{D}$ denotes the deformable convolution. We fuse the $\mathbf{F}_{Ftex}$ and $\mathbf{F}_{Dtex}$ through a convolution layer, obtaining the texture features $\mathbf{F}_{Tex}$. Through a decoder, we obtain the texture image $\mathbf{I}_{Tex}$. To extract the high-frequency detailed textures, the $\mathbf{I}_{Tex}$ is supervised by the residual of the HR image $\mathbf{I}_{HR}$ and the SISR image $\mathbf{I}_{SISR}$.

4.3. Adaptive Texture Transfer

To accurately combine the content of the SISR feature $\mathbf{F}_{SISR}$ and the textures of the reference feature $\mathbf{F}_{Tex}$, we design the adaptive texture transfer module to blend $\mathbf{F}_{Tex}$ and $\mathbf{F}_{SISR}$ according to the similarity between the two images.

To adaptively select the texture from $\mathbf{F}_{Tex}$, preventing the misaligned texture from deteriorating the output, we use the confidence map C calculated in Eq. (5) to suppress the weight of the misaligned texture region:

$$\mathbf{F}_{RefSR} = Conv(\mathbf{F}_{Tex}) \cdot C + \mathbf{F}_{SISR}, \tag{10}$$

where $Conv$ denotes a convolution layer. And then after eight residual blocks for restoration, we get the final output $\mathbf{I}_{RefSR}$. More details of confidence map C are discussed in the supplementary material.

4.4. Implementation Details

The overview network of the proposed framework is trained by two steps: 1) training of the singe image super-resolution network. 2) training of the texture extraction and transfer network.

Training of SISR Network. To ensure the content information of SISR results, we only use reconstruction loss, which is calculated by $\mathcal{L}_1$ loss, to train the SISR network. After training, we fix the SISR network.

Training of Texture Transfer Network. The super-resolution image $\mathbf{I}_{SISR}$ obtained from the SISR network is used for the feature alignment step. The texture transfer network has two outputs for supervision, the result of texture extraction $\mathbf{I}_{Tex}$ and the final result $\mathbf{I}_{RefSR}$. To let the network extract the high-frequency detailed texture information, we adopt the residual of the ground-truth image $\mathbf{I}_{HR}$ and $\mathbf{I}_{SISR}$ as supervision (More discussions of $\mathcal{L}_{rec}^{Tex}$ are in the the supplementary material.):

$$\mathcal{L}_{rec}^{Tex} = ||\mathbf{I}_{HR} - (\mathbf{I}_{SISR} + \mathbf{I}_{Tex})||_1, \tag{11}$$

As for the final output, we adopt reconstruction loss $\mathcal{L}_{rec}$, perceptual loss L_{per} [14] and adversarial loss L_{adv} [11]. The weight for L_{rec}, $\mathcal{L}_{per}$ and $\mathcal{L}_{adv}$ are 1, 10^{-2} and 10^{-4}, respectively. The initial training rate is set as 10^{-4}.

Table 1. **Quantitative Comparisons with the state-of-the-art methods.** We use PSNR/SSIM metrics for evaluation. The best and second-best performances are marked by **red** and blue colors, respectively. The RefSR models with '-*rec*' suffix are trained only by the reconstruction loss. Our proposed method outperforms significantly against current SISR and RefSR state-of-the-art methods.

	Method	CUFED5	Sun80	Urban100	Manga109	WR-SR
		PSNR/SSIM	PSNR/SSIM	PSNR/SSIM	PSNR/SSIM	PSNR/SSIM
SISR	SRCNN [10]	25.33/0.745	28.26/0.781	24.41/0.738	27.12/0.850	27.27/0.767
	EDSR [21]	25.93/0.777	28.52/0.792	25.51/0.783	28.93/0.891	28.07/0.793
	RRDB [33]	26.41/0.783	29.99/0.814	25.98/0.788	29.87/0.907	27.96/0.793
	RCAN [38]	26.33/0.781	29.97/0.814	25.99/0.787	30.11/0.908	27.91/0.793
	SRGAN [18]	24.40/0.702	26.76/0.725	24.07/0.729	25.12/0.802	26.21/0.728
	ENet [24]	24.24/0.695	26.24/0.702	23.63/0.711	25.25/0.802	25.47/0.699
	ESRGAN [33]	21.90/0.633	24.18/0.651	20.91/0.620	23.53/0.797	26.07/0.726
	RankSRGAN [37]	22.31/0.635	25.60/0.667	21.47/0.624	25.04/0.803	26.15/0.719
RefSR	CrossNet [41]	25.48/0.764	28.52/0.793	25.11/0.764	23.36/0.741	-
	SRNTT [40]	25.61/0.764	27.59/0.756	25.09/0.774	27.54/0.862	26.53/0.745
	SRNTT-*rec* [40]	26.24/0.784	28.54/0.793	25.50/0.783	28.95/0.885	27.59/0.780
	TTSR [36]	25.53/0.765	28.59/0.774	24.62/0.747	28.70/0.886	26.83/0.762
	TTSR-*rec* [36]	27.09/0.804	30.02/0.814	25.87/0.784	30.09/0.907	27.97/0.792
	MASA [22]	24.92/0.729	27.12/0.708	23.78/0.712	27.34/0.848	-
	MASA-*rec* [22]	27.54/0.814	30.15/0.815	26.09/0.786	30.28/0.909	-
	C^2-Matching [13]	27.16/0.805	29.75/0.799	25.52/0.764	29.73/0.893	27.80/0.780
	C^2-Matching-*rec* [13]	28.24/0.841	30.18/0.817	26.03/0.785	30.47/0.911	28.32/0.801
	Ours	27.37/0.816	28.85/0.768	25.80/0.776	30.12/0.889	27.40/0.769
	Ours-*rec*	**28.64/0.850**	**30.31/0.820**	**26.71/0.807**	**31.23/0.917**	**28.52/0.807**

Table 2. **Quantitative comparison at different levels on the CUFED5 testing set.** 'L1' is the most relevant reference and 'L4' is the least. 'LR' means directly using the LR image itself as the reference. For different reference levels, our method all obtains the best performance.

Method	L1	L2	L3	L4	LR
	PSNR/SSIM	PSNR/SSIM	PSNR/SSIM	PSNR/SSIM	PSNR/SSIM
CrossNet [41]	25.48/0.764	25.48/0.764	25.47/0.763	25.46/0.763	25.46/0.763
SRNTT-*rec* [40]	26.15/0.781	26.04/0.776	25.98/0.775	25.95/0.774	25.91/0.776
SSEN-*rec* [27]	26.78/0.791	26.52/0.783	26.48/0.782	26.42/0.781	-
CIMR-*rec* [35]	27.32/0.805	27.05/0.799	26.92/0.796	26.86/0.794	-
TTSR-*rec* [36]	26.99/0.800	26.74/0.791	26.64/0.788	26.58/0.787	26.43/0.782
MASA-*rec* [22]	27.35/0.814	26.92/0.796	26.82/0.793	26.74/0.790	26.59/0.784
C^2-Matching-*rec* [13]	28.24/0.841	27.39/0.813	27.17/0.806	26.94/0.799	26.53/0.784
Ours-*rec*	**28.64/0.850**	**27.77/0.821**	**27.46/0.815**	**27.23/0.807**	**26.83/0.794**

5. Experiments

5.1. Datasets and Metrics

Training datasets. The CUFED5 [40] training set consists of 11,871 image pairs, and each image pair has one HR image and one reference image both with the resolution of 160 × 160. We train our model with the scale factor x4.

Testing datasets. To evaluate our method, we adopt five benchmarks: CUFED5 [40] testing set, Sun80 [28], WR-SR [13], Urban100 [12] and Manga109 [23]. CUFED5 testing set consists of 126 image pairs, and each input image has 5 reference images with different similarity levels. Sun80 has 80 images, and each image has 20 reference images. WR-SR consists of 80 images, and each image has one reference image searched through Google Image. We evaluate our method on Urban100 and Manga109 following [13, 36, 40]. Urban100 has 100 building images with highly self-similarity, so we use LR images as the reference image. For Manga109 dataset, we randomly select HR images from the dataset as the reference image.

Evaluation metrics. The RefSR results are evaluated by metrics of PSNR and SSIM on Y channel of YCrCb space.

5.2. Comparison with State-of-the-art Methods

Quantitative Comparison. We compare the proposed method with the following SISR and RefSR methods. The SISR methods include SRCNN [10], EDSR [21], RCAN [38], SRGAN [18], ENet [24], ESRGAN [33]

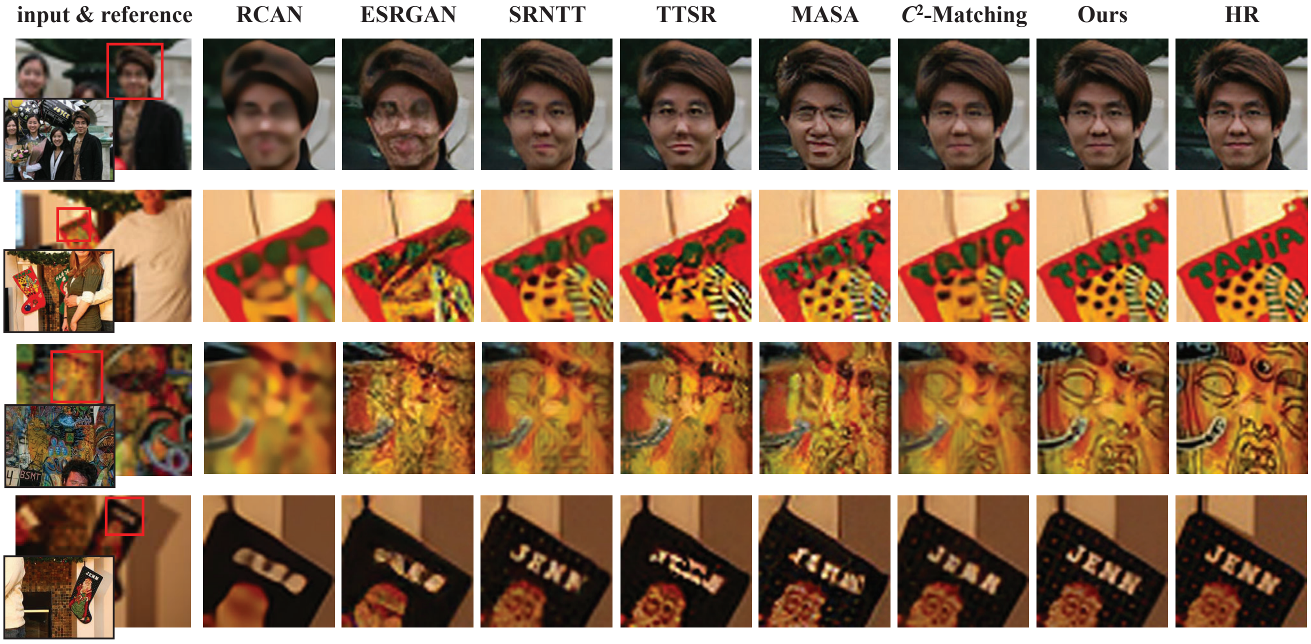

Figure 5. **Visual comparisons on the CUFED5 testing set.** We compare the proposed methods with 6 different SISR and Ref state-of-the-art methods. Among the methods, only RCAN is trained with l_1 loss, and others are all trained with GAN loss. Our method restores more realistic textures compared with other RefSR and SISR methods. **(Zoom-in for best view)**

and RankSRGAN [37]. As for RefSR methods, CrossNet [41], SRNTT [40], TTSR [36], MASA [22] and C^2-Mathcing [13] are included. C^2-Mathcing is the current state-of-the-art method recently, which achieves the best performance on both PSNR and SSIM.

Table 1 shows that our method outperforms existing state-of-the-art methods on all five datasets. The quantitative comparisons demonstrate that our proposed model has a significant improvement over 0.4dB compared with the state-of-the-art methods in standard CUFED5 benchmark.

Qualitative Evaluation. In Fig.5, we show the visual comparisons with state-of-the-art SISR and RefSR methods. Our method can achieve more pleasing visual quality with more detailed textures transferred from the reference HR images. As shown in the first row of the Fig.5, our method can restore the face with more realistic details. Besides, in the last row of Fig.5, our method obtains clear letters, while others generate artifacts or blurry results.

Robustness to irrelevant references. To evaluate the robustness to irrelevant references, we compare our method with other RefSR methods at different reference levels on the CUFED5 testing set. Table 2 shows the results of five relevant degrees. For different similarity levels, our method all achieves the best performance, which not only demonstrates our superiority on texture transfer, but also proves the robustness to irrelevant references of our method.

5.3. Ablation Studies

In this section, we conduct ablation studies on the two key components in our methods: (1) the task decoupled framework,(2) the texture extraction and transfer module.

Task decoupled framework. We set the model without the SISR part of our framework as the baseline, which achieves the super-resolution and texture transfer jointly through one single network. Table 3 evaluates the effectiveness of the task decoupled framework. **With similar reference**, we all get a gain over 0.26dB for RefSR datasets, CUFED5, Sun80 and WR-SR. Meanwhile, in Fig.6(a), the model with the decoupled framework can produce realistic images highly similar to the GT, with more textures and details transferred from the reference image. Both the quantitative evaluation and the qualitative comparison indicate that the task decoupled framework of the RefSR task can prompt the model to extract and transfer more textures from reference images. **Without similar reference**, as for SISR datasets, Urban100 and Manga109 datasets, Table 3 demonstrates that the decoupled framework achieves a significant boost over 1dB compared with baseline. Besides, Fig.6(b) shows that the baseline method can easily result in blur and artifacts, while our method with the decoupled framework alleviates the issue and obtains more details. The results prove that the task decoupled framework is more robust as irrelevant references are given. In conclusion, our framework effectively decouples the super-resolution task and the texture transfer task of RefSR, thus obtaining better performance.

Texture Extraction Module. Table 4 evaluates the effectiveness of flow-based alignment and deformable alignment in texture extraction module. We train the following variations. (A) baseline SISR without reference. (B) with

Table 3. **Quantitative evaluation for ablation study of the decouple framework.** The decouple framework brings an enormous improvement on the five datasets. Especially we obtain over 1dB improvement on Urban100 and Manga109.

Decouple	CUFED5	Sun80	Urban100	Manga109	WR-SR
w/o Decouple	28.36/0.842	30.01/0.812	25.66/0.769	29.98/0.901	28.16/0.797
w/ Decouple	**28.64/0.850**	**30.31/0.820**	**26.71/0.807**	**31.23/0.917**	**28.52/0.807**

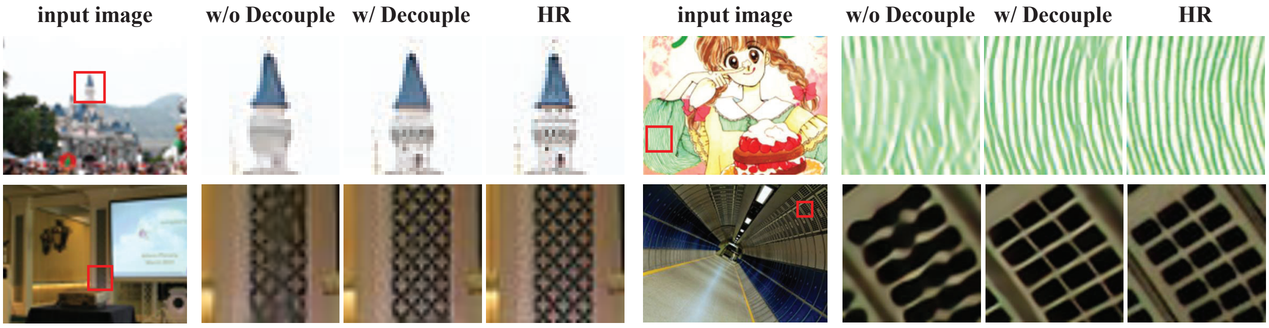

(a) Situation w/ similar reference content.

(b) Situation w/o similar reference content.

Figure 6. **Qualitative comparison for ablation study of the decouple framework.** (a) Situation with similar reference. The model with the decoupled framework results in more real textures transferred from reference. (b) Situation without similar reference. The model with decoupled framework can recover more details. **(Zoom-in for best view)**

Table 4. **Quantitative evaluation for ablation study of texture extraction and transfer modules.** The PSNR/SSIM is computed on CUFED5.

ID	Flow	DCN	ATT	PSNR/SSIM
(A)				26.41/0.783
(B)	✓			27.91/0.832
(C)		✓		28.29/0.843
(D)	✓	✓		28.50/0.848
(E)	✓	✓	✓	**28.64/0.850**

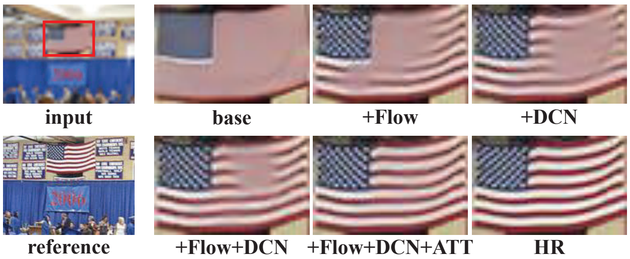

Figure 7. **Ablation study on texture extraction and transfer modules.**

flow-based (Flow) alignment. (C) with deformable convolution (DCN) alignment. (D) with both Flow and DCN alignment. (E) further with adaptive texture transfer(ATT).

Compared with (A), the setting (B) and (C) turn the SISR task into the RefSR task, with a gain over 1dB, due to the additional reference image. (C) has better performance than (B), indicating the superiority of deformable alignment against flow-based alignment in RefSR. As shown in Fig.7, the deformable alignment and the flow-based alignment can recover clear textures of different regions. Therefore, we combine the two alignment methods in the texture extraction module. As shown in Table 4, (D) achieves significant improvement compared with (B) and (C). Fig.7 also shows that results of (D) aggregate the realistic texture in (B) and (C). In conclusion, after combining the stability of flow-based alignment and the superiority of deformable alignment, the model obtains a better performance.

Adaptive Texture Transfer. As show in the last row in Table 4 and the result with "Flow+DCN+ATT" in Fig.7, the adaptive texture transfer module refines textures obtained from the texture extraction module and has a further gain of 0.14dB in PSNR on the standard CUFED5 benchmark.

6. Conclusion

In this paper, we first deeply investigate the reference-underuse issue and the reference-misuse issue for RefSR, which are due to the improper coupled framework design. Therefore, we propose a novel framework, decoupling the super-resolution task and the texture transfer task for RefSR. For the LR image, the super-resolution task coarsely upsamples the LR image only by LR itself. For the reference image, the texture transfer task extracts and transfers the realistic textures from the reference image. The texture extraction and the adaptive texture transfer modules are further proposed to migrate the textures more sufficiently. Extensive experiments on five benchmarks quantitatively and qualitatively demonstrate the superior performance of our proposed method over state-of-the-art methods.

Acknowledgements

This work was supported in part by Chinese National Key R&D Program (2019YFB1804304), State Key Laboratory of UHD Video and Audio Production and Presentation, BirenTech Research, Shanghai Key Laboratory of Digital Media Processing and Transmissions(STCSM 18DZ2270700) and 111 plan(BP0719010).

References

[1] Wenbo Bao, Wei-Sheng Lai, Chao Ma, Xiaoyun Zhang, Zhiyong Gao, and Ming-Hsuan Yang. Depth-aware video frame interpolation. In *IEEE Conf. Comput. Vis. Pattern Recog.*, pages 3703–3712, 2019. 5

[2] Wenbo Bao, Wei-Sheng Lai, Xiaoyun Zhang, Zhiyong Gao, and Ming-Hsuan Yang. Memc-net: Motion estimation and motion compensation driven neural network for video interpolation and enhancement. *IEEE Trans. Pattern Anal. Mach. Intell.*, 2019. 5

[3] Kelvin CK Chan, Xintao Wang, Ke Yu, Chao Dong, and Chen Change Loy. Basicvsr: The search for essential components in video super-resolution and beyond. In *IEEE Conf. Comput. Vis. Pattern Recog.*, pages 4947–4956, 2021. 5

[4] Kelvin CK Chan, Xintao Wang, Ke Yu, Chao Dong, and Chen Change Loy. Understanding deformable alignment in video super-resolution. In *AAAI*, 2021. 5

[5] Kelvin CK Chan, Shangchen Zhou, Xiangyu Xu, and Chen Change Loy. Basicvsr++: Improving video super-resolution with enhanced propagation and alignment. *IEEE Conf. Comput. Vis. Pattern Recog. Worksh.*, 2021. 5

[6] Yangdong Chen, Zhaolong Zhang, Yanfei Wang, Yuejie Zhang, Rui Feng, Tao Zhang, and Weiguo Fan. Ae-net: Fine-grained sketch-based image retrieval via attention-enhanced network. In *Pattern Recognition*, page 108291, 2022. 3

[7] Xianhang Cheng and Zhenzhong Chen. Multiple video frame interpolation via enhanced deformable separable convolution. *IEEE Trans. Pattern Anal. Mach. Intell.*, 2021. 5

[8] Jifeng Dai, Haozhi Qi, Yuwen Xiong, Yi Li, Guodong Zhang, Han Hu, and Yichen Wei. Deformable convolutional networks. In *Int. Conf. Comput. Vis.*, pages 764–773, 2017. 5

[9] Tao Dai, Jianrui Cai, Yongbing Zhang, Shu-Tao Xia, and Lei Zhang. Second-order attention network for single image super-resolution. In *IEEE Conf. Comput. Vis. Pattern Recog.*, pages 11065–11074, 2019. 2

[10] Chao Dong, Chen Change Loy, Kaiming He, and Xiaoou Tang. Image super-resolution using deep convolutional networks. *IEEE Trans. Pattern Anal. Mach. Intell.*, 38(2):295–307, 2015. 1, 2, 6

[11] Ishaan Gulrajani, Faruk Ahmed, Martin Arjovsky, Vincent Dumoulin, and Aaron C Courville. Improved training of wasserstein gans. In *Adv. Neural Inform. Process. Syst.*, pages 5767–5777, 2017. 5

[12] Jia-Bin Huang, Abhishek Singh, and Narendra Ahuja. Single image super-resolution from transformed self-exemplars. In *IEEE Conf. Comput. Vis. Pattern Recog.*, pages 5197–5206, 2015. 6

[13] Yuming Jiang, Kelvin C.K. Chan, Xintao Wang, Chen Change Loy, and Ziwei Liu. Robust reference-based super-resolution via C^2-matching. In *IEEE Conf. Comput. Vis. Pattern Recog.*, pages 2103–2112, 2021. 1, 3, 6, 7

[14] Justin Johnson, Alexandre Alahi, and Li Fei-Fei. Perceptual losses for real-time style transfer and super-resolution. In *Eur. Conf. Comput. Vis.*, pages 694–711, 2016. 2, 5

[15] Jiwon Kim, Jung Kwon Lee, and Kyoung Mu Lee. Accurate image super-resolution using very deep convolutional networks. In *IEEE Conf. Comput. Vis. Pattern Recog.*, pages 1646–1654, 2016. 2

[16] Jiwon Kim, Jung Kwon Lee, and Kyoung Mu Lee. Deeply recursive convolutional network for image super-resolution. In *IEEE Conf. Comput. Vis. Pattern Recog.*, pages 1637–1645, 2016. 1, 2

[17] Wei-Sheng Lai, Jia-Bin Huang, Narendra Ahuja, and Ming-Hsuan Yang. Deep laplacian pyramid networks for fast and accurate super-resolution. In *IEEE Conf. Comput. Vis. Pattern Recog.*, pages 624–632, 2017. 2

[18] Christian Ledig, Lucas Theis, Ferenc Huszár, Jose Caballero, Andrew Cunningham, Alejandro Acosta, Andrew Aitken, Alykhan Tejani, Johannes Totz, Zehan Wang, et al. Photo-realistic single image super-resolution using a generative adversarial network. In *IEEE Conf. Comput. Vis. Pattern Recog.*, pages 4681–4690, 2017. 2, 6

[19] Hyeongmin Lee, Taeoh Kim, Tae-young Chung, Daehyun Pak, Yuseok Ban, and Sangyoun Lee. Adacof: Adaptive collaboration of flows for video frame interpolation. In *IEEE Conf. Comput. Vis. Pattern Recog.*, pages 5316–5325, 2020. 5

[20] Zhen Li, Jinglei Yang, Zheng Liu, Xiaomin Yang, Gwanggil Jeon, and Wei Wu. Feedback network for image super-resolution. In *IEEE Conf. Comput. Vis. Pattern Recog.*, pages 3867–3876, 2019. 2

[21] Bee Lim, Sanghyun Son, Heewon Kim, Seungjun Nah, and Kyoung Mu Lee. Enhanced deep residual networks for single image super-resolution. In *IEEE Conf. Comput. Vis. Pattern Recog. Worksh.*, pages 1637–1645, 2016. 2, 6

[22] Liying Lu, Wenbo Li, Xin Tao, Jiangbo Lu, and Jiaya Jia. Masa-sr: matching acceleration and spatial adaptation for reference-based image super-resolution. In *IEEE Conf. Comput. Vis. Pattern Recog.*, pages 6368–6377, 2021. 1, 2, 3, 5, 6, 7

[23] Yusuke Matsui, Kota Ito, Yuji Aramaki, Azuma Fujimoto, Toru Ogawa, Toshihiko Yamasaki, and Kiyoharu Aizawa. Sketch-based manga retrieval using manga109 dataset. *Multimedia Tools and Applications*, 76(20):21811–21838, 2017. 6

[24] Mehdi SM Sajjadi, Bernhard Scholkopf, and Michael Hirsch. Enhancenet: Single image super-resolution through automated texture synthesis. In *Int. Conf. Comput. Vis.*, pages 4491–4500, 2017. 6

[25] Wang Shen, Wenbo Bao, Guangtao Zhai, Charlie L Wang, Jerry W Hu, and Zhiyong Gao. Prediction-assistant frame super-resolution for video streaming, 2021. *arXiv preprint arXiv:2103.09455*, 2021. 1

[26] Wenzhe Shi, Jose Caballero, Ferenc Husz´ar, Johannes Totz, Andrew P Aitken, Rob Bishop, Daniel Rueckert, and Zehan Wang. Real-time single image and video super-resolution using an efficient sub-pixel convolutional neural network. In *IEEE Conf. Comput. Vis. Pattern Recog.*, pages 1874–1883, 2016. 1, 2

[27] Gyumin Shim, Jinsun Park, , and In So Kweon. Robust reference-based super-resolution with similarity-aware de-

formable convolution. In *IEEE Conf. Comput. Vis. Pattern Recog.*, pages 8425–8434, 2020. 1, 2, 3, 6

[28] Libin Sun and James Hays. Super-resolution from internet-scale scene matching. In *IEEE Int. Conf. Comput. photo.*, pages 1–12, 2012. 6

[29] Ying Tai, Jian Yang, Xiaoming Liu, and Chunyan Xu. Memnet: A persistent memory network for image restoration. In *Int. Conf. Comput. Vis.*, pages 4539–4547, 2017. 2

[30] Yapeng Tian, Yulun Zhang, Yun Fu, and Chenliang Xu. Tdan: Temporally-deformable alignment network for video super-resolution. In *IEEE Conf. Comput. Vis. Pattern Recog.*, pages 3360–3369, 2020. 5

[31] Tengfei Wang, Jiaxin Xie, Wenxiu Sun, Qiong Yan, and Qifeng Chen. Dual-camera super-resolution with aligned attention modules. In *Int. Conf. Comput. Vis.*, pages 2001–2010, 2021. 1

[32] Xintao Wang, Kelvin CK Chan, Ke Yu, Chao Dong, and Chen Change Loy. Edvr: Video restoration with enhanced deformable convolutional networks. In *IEEE Conf. Comput. Vis. Pattern Recog. Worksh.*, 2019. 5

[33] Xintao Wang, Ke Yu, Shixiang Wu, Jinjin Gu, Yihao Liu, Chao Dong, Yu Qiao, and Chen Change Loy. Esrgan: Enhanced super-resolution generative adversarial networks. In *Eur. Conf. Comput. Vis. Worksh.*, 2018. 2, 4, 6

[34] Yanchun Xie, Jimin Xiao, Mingjie Sun, Chao Yao, and Kaizhu Huang. Feature representation matters: End-to-end learning for reference-based image super-resolution. In *Eur. Conf. Comput. Vis.*, pages 230–245. Springer, 2020. 2

[35] Xu Yan, Weibing Zhao, Kun Yuan, Ruimao Zhang, Zhen Li, and Shuguang Cui. Towards content-independent multi-reference super-resolution: Adaptive pattern matching and feature aggregation. In *Eur. Conf. Comput. Vis.*, pages 52–68, 2020. 2, 6

[36] Fuzhi Yang, Huan Yang, Jianlong Fu, Hongtao Lu, and Baining Guo. Learning texture transformer network for image super-resolution. In *IEEE Conf. Comput. Vis. Pattern Recog.*, pages 5791–5800, 2020. 1, 2, 3, 5, 6, 7

[37] Wenlong Zhang, Yihao Liu, Chao Dong, and Yu Qiao. Ranksrgan: Generative adversarial networks with ranker for image super-resolution. In *Int. Conf. Comput. Vis.*, pages 3096–3105, 2019. 2, 6, 7

[38] Yulun Zhang, Kunpeng Li, Kai Li, Lichen Wang, Bineng Zhong, and Yun Fu. Image super-resolution using very deep residual channel attention networks. In *Eur. Conf. Comput. Vis.*, pages 286–301, 2018. 1, 2, 6

[39] Yulun Zhang, Yapeng Tian, Yu Kong, Bineng Zhong, and Yun Fu. Residual dense network for image super-resolution. In *IEEE Conf. Comput. Vis. Pattern Recog.*, pages 2472–2481, 2018. 2

[40] Zhifei Zhang, ZhaowenWang, Zhe Lin, and Hairong Qi. Image super-resolution by neural texture transfer. In *IEEE Conf. Comput. Vis. Pattern Recog.*, pages 7982–7991, 2019. 1, 2, 3, 5, 6, 7

[41] Haitian Zheng, Mengqi Ji, Haoqian Wang, Yebin Liu, and Lu Fang. Crossnet: An end-to-end reference-based super resolution network using cross-scale warping. In *Eur. Conf. Comput. Vis.*, pages 88–104, 2018. 1, 2, 3, 6, 7